International Journal of Fuzzy Mathematics and Systems.
ISSN 2248-9940 Volume 16, Number 1 (2026), pp. 31-56

https://www.ripublication.com

A Neutrosophic Fuzzy Mathematics Approach for Uncertainty-Aware Tumor Growth Prediction

Induja Halder[1], Sushanta Man[2], and Subhendu Bikash Hazra[3]

[1]*Department of Mathematics, Bankura University, Bankura, 722155 West Bengal, India.*
[2]*Department of Mathematics, Bankura University, Bankura, 722155 West Bengal, India., E-mail:sushantazman@gmail.com*
[3]*Department of Mathematics, Bankura University, Bankura, 722155 West Bengal, India., E-mail:sbhazra@bankurauniv.ac.in*
[*]*Corresponding author: indujahalder789@gmail.com*

Abstract

Tumor growth is a highly dynamic biological process governed by the coupled effects of cell migration, diffusion, proliferation, and therapeutic response; all of which are subject to significant uncertainty arising from biological heterogeneity, patient-specific variability, and incomplete clinical information. Conventional advection–diffusion–reaction (ADR) models typically employ deterministic parameters and therefore provide limited capability for representing the uncertainty and indeterminacy inherent in tumor evolution. To overcome this limitation, this study develops a Neutrosophic Fuzzy Advection–Diffusion–Reaction Equation (NFADRE) in which the advection velocity, diffusion coefficient, and reaction rate are modeled as triangular neutrosophic numbers and represented through an (α, β, γ)-cut parametric framework. This formulation enables the simultaneous characterization of truth, indeterminacy, and falsity associated with the governing biological parameters, providing a mathematically consistent framework for uncertainty-aware tumor growth prediction. An explicit finite difference method is used to solve the proposed neutrosophic model. Numerical simulations are performed to investigate the influence of uncertain transport, diffusion, and reaction mechanisms on tumor progression. The results reveal that uncertainty in the reaction process predominantly governs long-term tumor evolution, whereas uncertainties in advection and diffusion primarily affect the migration speed and spatial invasion of tumor cells. Compared with the corresponding deterministic ADR model, the proposed neutrosophic formulation generates an uncertainty envelope that captures a spectrum of admissible tumor growth scenarios, thereby providing a richer and more informative description of tumor dynamics. The proposed framework offers an effective computational methodology for integrating uncertainty into tumor growth modeling and establishes a foundation for future research in patient-specific mathematical oncology, uncertainty quantification, and predictive computational

medicine.

Keywords and phrases: Neutrosophic Fuzzy Advection-diffusion-reaction equation, Finite difference Method, Tumor growth dynamics, Uncertainty analysis.

1. INTRODUCTION

Cancer remains one of the leading causes of morbidity and mortality worldwide and continues to pose a major challenge to modern healthcare systems. Among various forms of cancer, solid tumors exhibit highly complex growth dynamics governed by the interaction of multiple biological and physical processes, including cellular proliferation, migration, nutrient transport, extracellular matrix interactions, invasion, apoptosis, angiogenesis, immune response, and therapeutic interactions. The progression of a tumor is not only influenced by intrinsic cellular mechanisms but also by the surrounding microenvironment, where heterogeneous tissue properties, irregular vascular networks, and varying drug penetration significantly affect disease evolution. Consequently, understanding and accurately predicting tumor growth has become an important research area in mathematical biology, computational oncology, and biomedical engineering. Mathematical models capable of describing these coupled mechanisms provide valuable insights into tumor progression and offer a scientific basis for improving treatment planning, optimizing therapeutic strategies, and supporting personalized clinical decision-making. The advection–diffusion–reaction (ADR) equation is a widely used mathematical framework for modeling tumor growth by simultaneously describing directed cell migration, random diffusion, and biological reactions. However, conventional ADR models assume precisely known parameters, whereas the advection velocity, diffusion coefficient, and reaction rate are inherently uncertain due to biological variability, tissue heterogeneity, and incomplete clinical information. Consequently, incorporating uncertainty into this framework is essential for improving the reliability of tumor growth predictions.

To address uncertainty, fuzzy set theory introduced by Zadeh (1965)[28] has been widely adopted in mathematical modeling. Fuzzy models represent uncertain quantities through membership functions and have been successfully applied in medical diagnosis, engineering, optimization, and biological systems. In the context of differential equations, fuzzy-valued parameters enable the incorporation of imprecision arising from vague or incomplete information while preserving computational efficiency. However, classical fuzzy models describe uncertainty solely through a membership degree and therefore cannot explicitly distinguish between uncertainty caused by incomplete information and that arising from inconsistency or conflicting observations.

To overcome this limitation, intuitionistic fuzzy set theory was proposed by Atanassov (1986) [3], where each element is characterized by both membership and non-membership degrees, together with an implicitly defined hesitation margin. Intuitionistic fuzzy models provide greater flexibility than classical fuzzy models and

have been successfully applied to numerous decision-making and engineering problems involving uncertainty. Nevertheless, the hesitation degree is completely dependent on the membership and non-membership values, implying that it cannot be specified independently. As a result, intuitionistic fuzzy models remain inadequate for representing highly complex biological systems where uncertainty, inconsistency, and indeterminacy coexist independently due to conflicting experimental observations, missing clinical information, and patient-specific variability.

Neutrosophic set theory, introduced by Smarandache (1998)[21], extends both fuzzy and intuitionistic fuzzy theories by simultaneously incorporating three completely independent functions representing membership, indeterminacy, and non-membership. Unlike intuitionistic fuzzy sets, the indeterminacy component is treated as an independent quantity rather than being derived from the remaining two components. This additional degree of freedom enables neutrosophic theory to represent incomplete, inconsistent, vague, and contradictory information more realistically. Consequently, neutrosophic mathematics has gained considerable attention in optimization, artificial intelligence, image processing, medical diagnosis, decision sciences, and uncertain differential equations; demonstrating its capability to provide richer and more informative mathematical descriptions than deterministic or conventional fuzzy approaches. Furthermore, triangular neutrosophic numbers provide an efficient framework for representing uncertain model parameters while preserving the flexibility of neutrosophic theory (Smarandache, 1998 [21]; Wang et al., 2010 [27]).

The concept of fuzzy derivatives has been discussed by S. Seikkla [20]. Additionally, in [4] J. Buckley and T. Feuring proposed a method for solving elementary fuzzy partial differential equations.T. Allahviranloo in [2] used a numerical method to solve fuzzy PDEs based on Seikkla's definition of derivatives. Kermani and Saburi [14] used a numerical method for solving fuzzy differential equation. Furthermore, S. Man et al. utilized the finite difference method to solve the intuitionistic fuzzy heat equation in [17]. A boundary value problem of the second-order differential equation under the Neutrosophic fuzzy boundary condition has been solved using the finite difference method in [13]. As Neutrosophic fuzzy sets are more general and flexible than previous set theories, they can effectively capture and propagate uncertainty in PDEs, leading to more accurate solutions. Over the last decade, several researchers have proposed efficient numerical methods for solving ADR equations. For example, Tsega (2024)[26] developed a Crank–Nicolson finite difference scheme for nonlinear ADR equations with variable coefficients and established its stability and convergence properties, demonstrating its suitability for complex transport problems. Similarly, recent reaction–diffusion tumor models have incorporated heterogeneous diffusion coefficients, nonlinear growth kinetics, and stability analysis to better describe tumor progression under biologically realistic conditions (Alabdrabalnabi and Ali, 2024 [1]). Mathematical modeling has played a fundamental role in understanding tumor growth and invasion for several decades. One of the earliest mathematical descriptions of biological population propagation was proposed by Fisher (1937)[9], where reaction–diffusion equation became the foundation for modeling the spread of living cell populations. Later,

Tracqui (1995)[25] introduced one of the earliest mathematical model for glioma invasion by coupling diffusion with cellular proliferation, while Cruywagen et al. (1995)[8] formulated diffusion-based mathematical models capable of reproducing the infiltrative behavior of malignant brain tumors. Swanson et al. (2000, 2003)[23],[24] further refined these models by incorporating patient-specific diffusion and proliferation parameters, demonstrating that reaction–diffusion equations could accurately predict glioma growth observed in clinical imaging. Harpold et al. (2007)[12] comprehensively reviewed mathematical models of glioma growth and emphasized that reaction–diffusion frameworks provide valuable insight into tumor invasion, treatment planning, and disease progression. More recently, Byrne (2010)[5] highlighted the increasing importance of mathematical oncology and discussed the integration of biological mechanisms, computational methods, and clinical data into predictive cancer models.

In tumor-growth modeling, Rivaz et al. (2018)[19] proposed a fully fuzzy mathematical model for tumor growth based on fuzzy integro-partial differential equations, demonstrating that fuzzy representations more realistically capture uncertainty associated with cancer stem-cell dynamics and tumor-growth paradoxes. More recently, Khaliq et al. (2022) [15] developed fuzzy exponential, logistic, and Gompertz tumor-growth models using generalized Hukuhara differentiability and showed that fuzzy-valued parameters significantly improve the realism of tumor-growth prediction compared with crisp models. In their subsequent work Khaliq et al. (2023) [16] further extended the Gompertz tumor-growth model with the Allee effect under a fuzzy environment. These studies demonstrated that fuzzy-valued parameters provide more realistic predictions of tumor evolution than deterministic models. Furthermore, Zureigat et al. (2024)[30] proposed a fuzzy fractional cancer tumor model solved by an implicit finite difference method and showed that incorporating fuzzy uncertainty improves the representation of biological variability. More recently, Qayyum et al. (2025)[18] developed a hybrid computational framework for fractional cancer diffusion models under uncertainty by representing model parameters with triangular fuzzy numbers. Using a He–Laplace hybrid algorithm, they obtained accurate approximate solutions and demonstrated that fuzzy-fractional formulations provide a more realistic representation of tumor heterogeneity and parameter uncertainty than deterministic models. In addition, Georgieva et al. (2025)[11] introduced a double fuzzy integral transform for solving fuzzy advection–diffusion equations, whereas Gazi et al. (2025) [10] comprehensively reviewed recent advances in fuzzy differential equations, including generalized Hukuhara differentiability, transform methods, finite difference techniques, and fractional fuzzy models, highlighting their growing applications in engineering and biomedical sciences. Extending these developments, Zureigat et al. (2026)[31] presented one of the first comprehensive analytical and numerical investigations of the neutrosophic fuzzy advection–diffusion equation using triangular neutrosophic numbers and finite difference methods, demonstrating accurate numerical approximations while explicitly preserving neutrosophic uncertainty.

Despite recent advances in neutrosophic numerical methods, their application to tumor growth models governed by advection–diffusion–reaction equations remains limited.

Most existing studies emphasize transport phenomena, while uncertainty in the reaction process has received comparatively little attention. This motivates the development of a neutrosophic ADR framework that consistently incorporates uncertainty into all governing mechanisms of tumor evolution.

The principal contributions of this work are summarized as follows. First, a novel Neutrosophic Fuzzy Advection–Diffusion–Reaction equation (NADRE) is formulated for tumor growth prediction by representing the governing transport and reaction parameters through triangular neutrosophic numbers. Second, an (α, β, γ)-cut parametric framework is developed to transform the neutrosophic problem into computationally tractable interval systems while preserving the truth, indeterminacy, and falsity characteristics of the original model. Third, an explicit finite difference scheme is constructed for the numerical approximation of the proposed model, providing an efficient computational tool for solving the resulting neutrosophic equations. Finally, extensive numerical investigations demonstrate how uncertainty associated with advection, diffusion, and particularly the reaction mechanism influences tumor migration, spatial invasion, and long-term growth dynamics. The proposed framework therefore establishes a mathematically consistent and computationally efficient methodology for integrating neutrosophic uncertainty into tumor growth modeling and provides a foundation for future developments in uncertainty quantification, predictive mathematical oncology, and patient-specific computational medicine.

2. PRELIMINARY CONCEPTS

In this section, we introduce the essential definitions, and notations that will be used throughout the paper.

Definition 2.1. Neutrosophic Fuzzy Sets (NFS): Let X be a universel set. A NFS A on X is defined as

$$A = \{\langle x, T_A(x), I_A(x), F_A(x)\rangle \mid x \in X\}, \tag{1}$$

where the functions $T_A : X \mapsto [0, 1]$, $I_A : X \mapsto [0, 1]$ and $F_A : X \mapsto [0, 1]$ represent the degree of membership, degree of indeterminacy and degree of non-membership respectively of the element $x \in X$ to the set A such that $0 \leq T_A(x) + I_A(x) + F_A(x) \leq 3$[22].

Definition 2.2. (α, β, γ)**-cuts:** As defined in [13] the (α, β, γ)-cuts are fixed values on A, where $\alpha, \beta, \gamma \in [0, 1]$ are fixed numbers such that $\alpha + \beta + \gamma \leq 3$ defined as

$$\{A_{\alpha,\beta,\gamma} = \{\langle T_A(x), I_A(x), F_A(x)\rangle : x \in X, T_A(x) \geq \alpha,\ I_A(x) \leq \beta, F_A(x) \leq \gamma\}. \tag{2}$$

Definition 2.3. Neutrosophic Number: A neutrosophic set A on a universal set of real numbers R is said to be neutrosophic number if it has the following properties[13]

1. A is normal if there exists $x_0 \in \mathbb{R}$ such that $T_A(x_0) = 1, I_A(x_0) = F_A(x_0) = 0$
2. A is convex for the membership function T_A
   i.e., $T_A(\lambda x_1 + (1 - \lambda)x_2) \geq \min\{T_A(x_1),\ T_A(x_2);\ \forall x_1, x_2 \in \mathbb{R},\ \lambda \in [0, 1]\}$

3. A is concave for the indeterministic I_A and the non-membership function F_A i.e., $I_A(\lambda x_1 + (1-\lambda)x_2) \geq \min\{I_A(x_1),\ I_A(x_2)\};\ \forall x_1, x_2 \in \mathbb{R},\ \lambda \in [0,1]\}$, and $F_A(\lambda x_1 + (1-\lambda)x_2) \geq \max\{F_A(x_1),\ F_A(x_2)\};\ \forall x_1, x_2 \in \mathbb{R},\ \lambda \in [0,1]\}$.

Definition 2.4. Triangular Single valued Neutrosophic Number (TrSVNN):[6] A triangular single valued neutrosophic number $\tilde{A}$ is denoted by $\tilde{A} = \langle (p_1, p_2, p_3), (q_1, q_2, q_3), (r_1, r_2, r_3) \rangle$ whose membership, indeterminacy and non-membership functions are defined as follows:

$$T_{\tilde{A}}(x) = \begin{cases} \frac{x-p_1}{p_2-p_1}, & \text{for } p_1 \leq x < p_2 \\ 1, & \text{for } x = p_2 \\ \frac{p_3-x}{p_3-p_2}, & \text{for } p_2 < x \leq p_3 \\ 0, & \text{otherwise} \end{cases} \tag{3}$$

$$I_{\tilde{A}}(x) = \begin{cases} \frac{q_2-x}{q_2-q_1}, & \text{for } q_1 \leq x < q_2 \\ 0, & \text{for } x = q_2 \\ \frac{x-q_2}{q_3-q_2}, & \text{for } q_2 < x \leq q_3 \\ 1, & \text{otherwise} \end{cases} \tag{4}$$

and

$$F_{\tilde{A}}(x) = \begin{cases} \frac{r_2-x}{r_2-r_1}, & \text{for } r_1 \leq x < r_2 \\ 0, & \text{for } x = r_2 \\ \frac{x-r_2}{r_3-r_2}, & \text{for } r_2 < x \leq r_3 \\ 1, & \text{otherwise} \end{cases} \tag{5}$$

where $0 \leq T_{\tilde{A}}(x) + I_{\tilde{A}}(x) + F_{\tilde{A}}(x) \leq 3, x \in \tilde{A}$.

The (α, β, γ)-cut of $\tilde{A} = \langle (p_1, p_2, p_3), (q_1, q_2, q_3), (r_1, r_2, r_3) \rangle$ can be represented as

$$\tilde{A}_{\alpha,\beta,\gamma} = \langle [A_T^L(\alpha), A_T^U(\alpha)], [A_I^L(\beta), A_I^U(\beta)], [A_F^L(\gamma), A_F^U(\gamma)] \rangle, \tag{6}$$

where

$$A_T^L(\alpha) = p_1 + \alpha(p_2 - p_1),$$

$$A_T^U(\alpha) = p_3 - \alpha(p_3 - p_2),$$

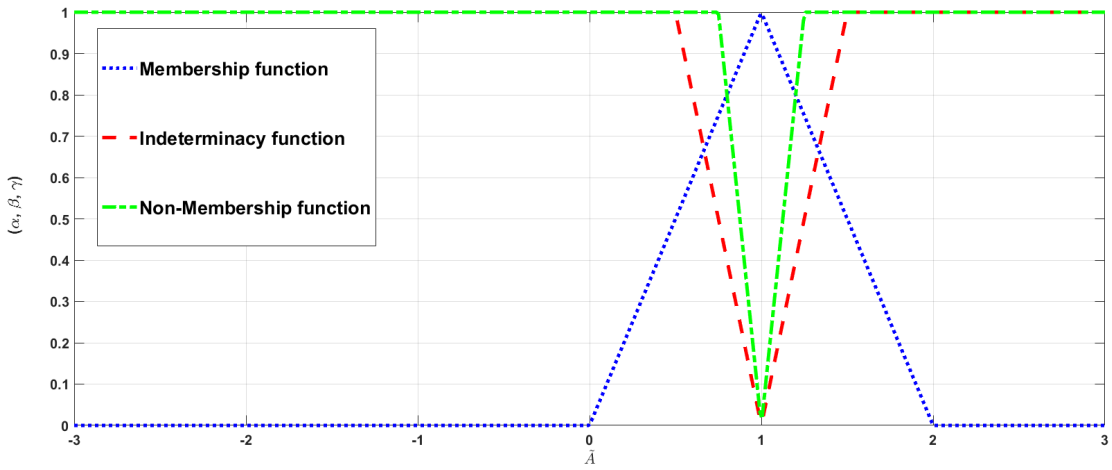

Figure 1: Graphical representation of TrSVNN

$$A_I^L(\beta) = q_2 - \beta(q_2 - q_1),$$

$$A_I^U(\beta) = q_2 + \beta(q_3 - q_2),$$

$$A_F^L(\gamma) = r_2 - \gamma(r_2 - r_1),$$

$$A_F^U(\gamma) = r_2 + \gamma(r_3 - r_2).$$

3. NEUTROSOPHIC FUZZY ADVECTION-DIFFUSION-REACTION EQUATION

To describe tumor cell migration, cellular diffusion, and treatment response under uncertain physiological conditions, we propose a Neutrosophic Fuzzy Advection–Diffusion–Reaction Equation (NFADRE) defined over an infinite spatial domain. In this formulation, the advection velocity, diffusion coefficient, and reaction coefficient are represented by triangular neutrosophic numbers, allowing the model to account for biological variability, incomplete clinical information, and indeterminate treatment response.
The governing equation is: [7]

$$\frac{\partial C}{\partial t} = \tilde{D}\frac{\partial^2 C}{\partial x^2} - \tilde{u}\frac{\partial C}{\partial x} - \tilde{\lambda}C, \qquad -\infty < x < \infty, \quad t > 0, \tag{7}$$

with the initial condition

$$C(x, 0) = C_0(x), \tag{8}$$

and the boundary conditions

$$\lim_{x\to-\infty} C(x,t) = 0, \qquad t > 0, \tag{9}$$

$$\lim_{x\to+\infty} C(x,t) = 0, \qquad t > 0. \tag{10}$$

- **Initial distribution:** $C(x,0) = C_0(x)$, defines the tumor distribution at the initial time and serves as the starting point for the temporal evolution governed by equation (7).

- **Boundary Conditions:** The boundary conditions specify the interaction of the tumor with the surrounding environment at the edges of the computational domain. The above conditions (9) and (10) imply that the tumor cell concentration approaches zero as the distance from the primary tumor region becomes sufficiently large. Biologically, this assumption reflects the fact that tumor cells are initially localized within a finite region of tissue, and although advection and diffusion cause spatial spreading over time, the concentration remains negligible far from the tumor site.

Furthermore,

- $C(x,t)$ denotes the concentration of the tumor cell at spatial location x and time t.

- $\frac{\partial C}{\partial t}$ indicates the temporal rate of change of the tumor cell concentration.

- $\tilde{u}$ represents the neutrosophic advection velocity describing the directed migration of tumor cells due to physiological transport mechanisms such as interstitial fluid flow and tissue movement.

- $\frac{\partial C}{\partial x}$ denotes the first-order spatial derivative describing the concentration gradient responsible for directional cell transport.

- $\tilde{D}$ is the neutrosophic diffusion coefficient representing the random dispersion of tumor cells into the surrounding tissue.

- The second order spatial derivative $\frac{\partial^2 C}{\partial x^2}$ accounts for the diffusion of tumor cells within the surrounding tissue.

- $\tilde{\lambda}$ denotes the neutrosophic reaction coefficient describing the net biological effect of tumor cell proliferation, apoptosis, immune response, and treatment-induced cell death.

3.1. Neutrosophic Representation of the Model Parameters

In the proposed NFADRE model, the uncertain transport and reaction coefficients are expressed as triangular neutrosophic numbers (TNNs) to systematically represent uncertainty in the governing parameters. Each parameter is described by three independent membership functions corresponding to the degrees of truth, indeterminacy, and falsity, allowing uncertainty to be incorporated directly into the mathematical formulation.

Accordingly, the neutrosophic model parameters $\tilde{u}, \tilde{D}$ and $\tilde{\lambda}$, are characterized by their respective membership functions $T_{\tilde{u}}$,$T_{\tilde{D}}$ and $T_{\tilde{\lambda}}$; the indeterminacy functions $I_{\tilde{u}}$, $I_{\tilde{D}}$ and $I_{\tilde{\lambda}}$; and the non-membership functions $F_{\tilde{u}}$, $F_{\tilde{D}}$ and $F_{\tilde{\lambda}}$.

Here, the membership function indicates the degree of confidence associated with a parameter value, the indeterminacy function reflects the level of uncertainty resulting from incomplete or ambiguous information, and the non-membership function represents the degree to which the parameter value is not supported by the available evidence. Together, these three components provide a comprehensive mathematical framework for representing uncertain parameters in the proposed NFADRE model.

3.2. Parametric Representation by the (α, β, γ)-Cut

For numerical computation, the triangular neutrosophic parameters are converted into their corresponding interval-valued representations using the (α, β, γ)-cut approach.

For $\alpha, \beta, \gamma \in [0, 1]$, where α, β, and γ denote the truth, indeterminacy, and falsity levels, respectively, satisfying $0 \leq \alpha, \beta, \gamma \leq 1$, such that $\alpha + \beta + \gamma \leq 3$.

The (α, β, γ)-cut representations of the neutrosophic parameters are given by

$$\tilde{u}[\alpha, \beta, \gamma] = \langle [u_T^L(\alpha), u_T^U(\alpha)], [u_I^L(\beta), u_I^U(\beta)], [u_F^L(\gamma), u_F^U(\gamma)] \rangle,$$

$$\tilde{D}[\alpha, \beta, \gamma] = \langle [D_T^L(\alpha), D_T^U(\alpha)], [D_I^L(\beta), D_I^U(\beta)], [D_F^L(\gamma), D_F^U(\gamma)] \rangle$$

and

$$\tilde{\lambda}[\alpha, \beta, \gamma] = \langle [\lambda_T^L(\alpha), \lambda_T^U(\alpha)], [\lambda_I^L(\beta), \lambda_I^U(\beta)], [\lambda_F^L(\gamma), \lambda_F^U(\gamma)] \rangle.$$

Here, the lower and upper bounds of each interval are obtained from the corresponding triangular neutrosophic membership, indeterminacy and non-membership functions. As the values of α, β, and γ vary over their admissible ranges, a family of interval-valued coefficients is generated. Substituting these interval coefficients into the governing NFADRE produces a corresponding family of deterministic advection–diffusion–reaction equations, which are solved numerically using the proposed explicit finite difference scheme. This transformation preserves the neutrosophic uncertainty while providing a computationally efficient framework for numerical analysis.

Using that parameterization, equation (7) can be decomposed as:

$$\frac{\partial C}{\partial t} = D_T^L(\alpha)\frac{\partial^2 C}{\partial x^2} - u_T^L(\alpha)\frac{\partial C}{\partial x} - \lambda_T^L(\alpha)C, \tag{11}$$

$$\frac{\partial C}{\partial t} = D_T^U(\alpha)\frac{\partial^2 C}{\partial x^2} - u_T^U(\alpha)\frac{\partial C}{\partial x} - \lambda_T^U(\alpha)C, \tag{12}$$

$$\frac{\partial C}{\partial t} = D_I^L(\beta)\frac{\partial^2 C}{\partial x^2} - u_I^L(\beta)\frac{\partial C}{\partial x} - \lambda_I^L(\beta)C, \tag{13}$$

$$\frac{\partial C}{\partial t} = D_I^U(\beta)\frac{\partial^2 C}{\partial x^2} - u_I^U(\beta)\frac{\partial C}{\partial x} - \lambda_I^U(\beta)C, \tag{14}$$

$$\frac{\partial C}{\partial t} = D_F^L(\gamma)\frac{\partial^2 C}{\partial x^2} - u_F^L(\gamma)\frac{\partial C}{\partial x} - \lambda_F^L(\gamma)C, \tag{15}$$

$$\frac{\partial C}{\partial t} = D_F^U(\gamma)\frac{\partial^2 C}{\partial x^2} - u_F^U(\gamma)\frac{\partial C}{\partial x} - \lambda_F^U(\gamma)C. \tag{16}$$

3.3. Discretization using Finite Difference Method

Equations (11)–(16) are now linear (crisp) constant coefficient partial differential equations, more precisely advective diffusive and reactive equations. We use forward in time, backward in space for the advection term and central in space for diffusion (FTBSCS) term finite difference scheme to discritize the equations. To do that, we subdivide the x-t plane into sets of equal rectangles of sides $\delta x = h$, $\delta t = k$, by equally spaced grid lines parallel to t-axis, defined by $x_j = jh, j = 0, 1, 2, ...J$ and equally spaced grid lines parallel to x-axis, defined by $t_n = nk, n = 0, 1, 2, ...N$. The discrete dependent variable on the grid points is represented as $[C(x,t)]_{j,n} = C(x_j, t_n) = C_{j,n}$.

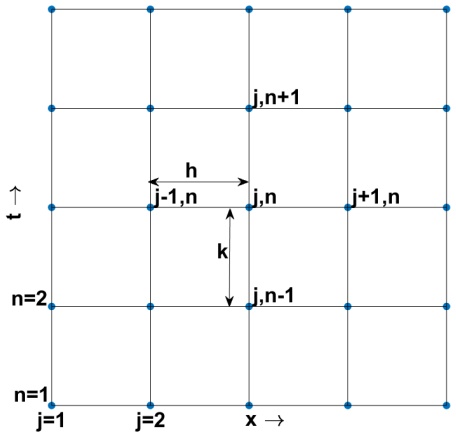

Figure 2: Grid

Using Taylor's theorem and definition of standard finite difference formula, we obtain:

$$\left(\frac{\partial C}{\partial t}\right)_{j,n} = \frac{C_{j,n+1} - C_{j,n}}{k} + O(k)(\text{Forward difference in time}), \tag{17}$$

$$\left(\frac{\partial C}{\partial x}\right)_{j,n} = \frac{C_{j,n} - C_{j-1,n}}{h} + O(h)(\text{Backward difference in space, upwinding}), \tag{18}$$

$$\left(\frac{\partial^2 C}{\partial x^2}\right)_{j,n} = \frac{C_{j+1,n} - 2C_{j,n} + C_{j-1,n}}{h^2} + O(h^2)(\text{Central difference in space}). \tag{19}$$

Substituting the discretized derivatives into the equations (11)–(16), neglecting the error terms, we get:

$$\frac{C_{j,n+1} - C_{j,n}}{k} = D_T^L(\alpha)\frac{C_{j+1,n} - 2C_{j,n} + C_{j-1,n}}{h^2} - u_T^L(\alpha)\frac{C_{j,n} - C_{j-1,n}}{h} - \lambda_T^L(\alpha)C_{j,n}, \tag{20}$$

$$\frac{C_{j,n+1} - C_{j,n}}{k} = D_T^U(\alpha)\frac{C_{j+1,n} - 2C_{j,n} + C_{j-1,n}}{h^2} - u_T^U(\alpha)\frac{C_{j,n} - C_{j-1,n}}{h} - \lambda_T^U(\alpha)C_{j,n}, \tag{21}$$

$$\frac{C_{j,n+1} - C_{j,n}}{k} = D_I^L(\beta)\frac{C_{j+1,n} - 2C_{j,n} + C_{j-1,n}}{h^2} - u_I^L(\beta)\frac{C_{j,n} - C_{j-1,n}}{h} - \lambda_I^L(\beta)C_{j,n}, \tag{22}$$

$$\frac{C_{j,n+1} - C_{j,n}}{k} + u_I^U(\beta)\frac{C_{j,n} - C_{j-1,n}}{h} = D_I^U(\beta)\frac{C_{j+1,n} - 2C_{j,n} + C_{j-1,n}}{h^2} - \lambda_I^U(\beta)C_{j,n}, \tag{23}$$

$$\frac{C_{j,n+1}-C_{j,n}}{k}=D_F^L(\gamma)\frac{C_{j+1,n}-2C_{j,n}+C_{j-1,n}}{h^2}-u_F^L(\gamma)\frac{C_{j,n}-C_{j-1,n}}{h}-\lambda_F^L(\gamma)C_{j,n}, \quad ,(24)$$

$$\frac{C_{j,n+1}-C_{j,n}}{k}=D_F^U(\gamma)\frac{C_{j+1,n}-2C_{j,n}+C_{j-1,n}}{h^2}-u_F^U(\gamma)\frac{C_{j,n}-C_{j-1,n}}{h}-\lambda_F^U(\gamma)C_{j,n}, \quad .(25)$$

Rearranging the equation to solve for the Neutrosophic fuzzy concentration, we have the scheme

$$C_{j,n+1}=C_{j,n}+\frac{D_T^L(\alpha)k}{h^2}(C_{j+1,n}-2C_{j,n}+C_{j-1,n})-\frac{u_T^L(\alpha)k}{h}(C_{j,n}-C_{j-1,n})-\lambda_T^L(\alpha)kC_{j,n}, \quad (26)$$

$$C_{j,n+1}=C_{j,n}+\frac{D_T^U(\alpha)k}{h^2}(C_{j+1,n}-2C_{j,n}+C_{j-1,n})-\frac{u_T^U(\alpha)k}{h}(C_{j,n}-C_{j-1,n})-\lambda_T^U(\alpha)kC_{j,n}, \quad (27)$$

$$C_{j,n+1}=C_{j,n}+\frac{D_I^L(\beta)k}{h^2}(C_{j+1,n}-2C_{j,n}+C_{j-1,n})-\frac{u_I^L(\beta)k}{h}(C_{j,n}-C_{j-1,n})-\lambda_I^L(\beta)kC_{j,n}, \quad (28)$$

$$C_{j,n+1}=C_{j,n}+\frac{D_I^U(\beta)k}{h^2}(C_{j+1,n}-2C_{j,n}+C_{j-1,n})-\frac{u_I^U(\beta)k}{h}(C_{j,n}-C_{j-1,n})-\lambda_I^U(\beta)kC_{j,n}, \quad (29)$$

$$C_{j,n+1}=C_{j,n}+\frac{D_F^L(\gamma)k}{h^2}(C_{j+1,n}-2C_{j,n}+C_{j-1,n})-\frac{u_F^L(\gamma)k}{h}(C_{j,n}-C_{j-1,n})--\lambda_F^L(\gamma)kC_{j,n}, \quad (30)$$

$$C_{j,n+1}=C_{j,n}+\frac{D_F^U(\gamma)k}{h^2}(C_{j+1,n}-2C_{j,n}+C_{j-1,n})-\frac{u_F^U(\gamma)k}{h}(C_{j,n}-C_{j-1,n})-\lambda_F^U(\gamma)kC_{j,n}, \quad (31)$$

with $j=0,1,2,...,J$ and $n=0,1,2,...,N$.

4. NUMERICAL EXAMPLE

To demonstrate the applicability and effectiveness of the proposed Neutrosophic Fuzzy Advection–Diffusion–Reaction Equation (NFADRE), a representative numerical example describing the spatio-temporal evolution of tumor cells is considered. The governing equation is solved using the proposed explicit finite difference method. The numerical experiment is designed to illustrate the combined effects of advection, diffusion, and reaction under parameter uncertainty while validating the accuracy and stability of the proposed computational approach.

Example: For the numerical simulation, we consider the growth of tumor cells in an unbounded domain governed by the one-dimensional Neutrosophic Fuzzy Advection–Diffusion–Reaction Equation. The governing equation is

$$\frac{\partial C}{\partial t} = \tilde{D}\frac{\partial^2 C}{\partial x^2} - \tilde{u}\frac{\partial C}{\partial x} - \tilde{\lambda}C, \quad -\infty < x < \infty, t > 0, \tag{32}$$

where $C(x,t)$ denotes the tumor cell concentration.

- **Initial distribution:** The initial distribution is assumed to be a Gassian Approximation of the Dirac delta function,

$$C(x,0) = \frac{1}{\varepsilon\sqrt{\pi}} \exp\left(-\frac{x^2}{\varepsilon^2}\right), \tag{33}$$

where $(\varepsilon > 0)$ is a small parameter controlling the width of the initial tumor profile. This initial condition represents a highly localized tumor centered at the origin while preserving the total initial tumor mass,

$$\int_{-\infty}^{\infty} \delta_\varepsilon(x)dx = 1 \tag{34}$$

- **Boundary Conditions:** Since the mathematical model is defined on an infinite domain, the boundary conditions are given by:

$$\lim_{x\to\pm\infty} C(x,t) = 0, \qquad t > 0. \tag{35}$$

For numerical implementation, the infinite domain is truncated to the finite spatial computational interval [-100,100], which is sufficiently large that the tumor concentration remains negligible at the computational boundaries throughout the simulation.
The uncertain coefficients are represented by triangular neutrosophic numbers $\tilde{u}$, $\tilde{D}$ and $\tilde{\lambda}$ and are parameterized using (α,β,γ)-cut representation as follows:

$$\tilde{u}[\alpha,\beta,\gamma] = \langle[\alpha, 2-\alpha], [1-0.5\beta, 1+0.5\beta], [1-0.25\gamma, 1+0.25\gamma]\rangle, \tag{36}$$

$$\tilde{D}[\alpha,\beta,\gamma] = \langle[0.75+0.25\alpha, 1.25-0.25\alpha], [1-0.75\beta, 1+0.75\beta], [1-0.5\gamma, 1+0.5\gamma]\rangle \tag{37}$$

and

$$\tilde{\lambda}[\alpha,\beta,\gamma] = \langle[0.05\alpha, 0.1-0.05\alpha], [1-0.85\beta, 1+0.85\beta], [1-0.15\gamma, 1+0.15\gamma]\rangle. \tag{38}$$

The resulting deterministic equations are solved by the explicit finite difference scheme developed in the previous section. The numerical solutions are presented at t=6, 12, and 24 months to examine the influence of uncertainty on tumor transport, diffusion, and treatment-induced decay. The obtained solution profiles illustrate the evolution of the tumor concentration over time and demonstrate the capability of the proposed neutrosophic framework to quantify the range of possible tumor behaviors arising from uncertain biological parameters.

Results and Discussion

This section presents the numerical results of the proposed explicit finite difference scheme for the Neutrosophic Fuzzy Advection–Diffusion–Reaction Equation (NFADRE) through a series of numerical experiments. Simulations are carried out under different (α, β, γ)-cut levels to examine the influence of neutrosophic uncertainty on the evolution of tumor cell concentration. The computed membership, indeterminacy, and non-membership concentration profiles are analyzed at selected time instances to assess the impact of uncertain transport and reaction parameters on the predicted tumor dynamics. Furthermore, the numerical results demonstrate the robustness of the proposed formulation in capturing parameter uncertainty while maintaining stable and consistent solution behavior. The observed trends and their physical interpretations are presented with the support of the corresponding figures and tables.

We present the results of our computations in the following figures.

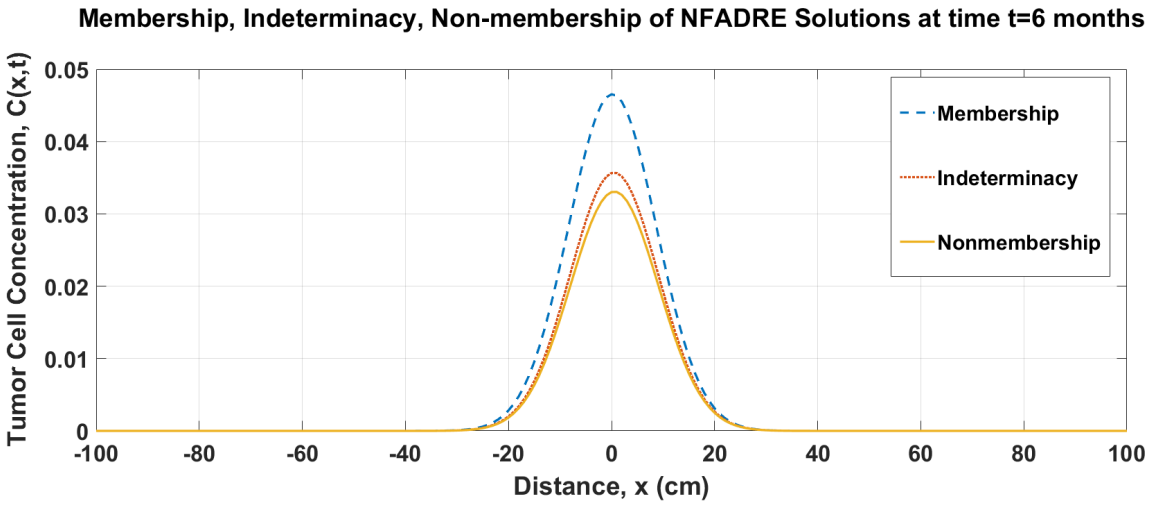

Figure 3: Cell Concentration using NFADRE at t=6 months for $\alpha = 0.3, \beta = 0.3, \gamma = 0.3$

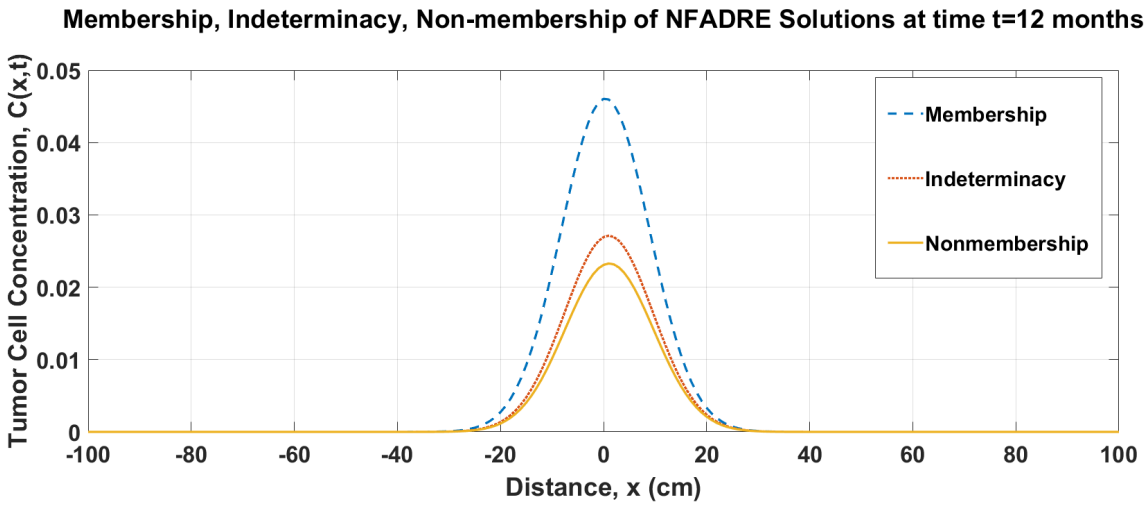

Figure 4: Cell Concentration using NFADRE at t=12 months for $\alpha = 0.3, \beta = 0.3, \gamma = 0.3$

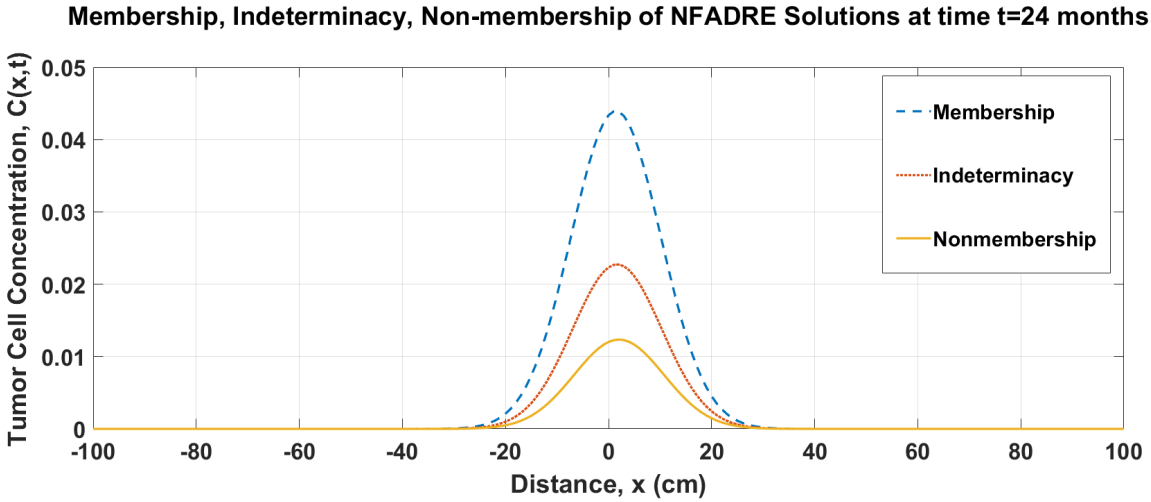

Figure 5: Cell Concentration using NFADRE at t=24 months for $\alpha = 0.3, \beta = 0.3, \gamma = 0.3$

The figures (3), (4), and (5) present the concentration distributions corresponding to the (α, β, γ)-cut level (0.3,0.3,0.3) at t=6, 12, and 24 months. At t=6 months, the tumor concentration remains highly localized around the initial position with a pronounced peak, indicating that diffusion has not yet produced significant spreading. The concentration profile exhibits a slight displacement in the positive spatial direction due to the advection process, while the reaction term begins to reduce the concentration through decay. As time progresses to t=12 months, diffusion becomes increasingly dominant, resulting in a broader spatial distribution and a noticeable reduction in the peak concentration. By t=24 months, the tumor profile has spread over a considerably larger region with

a substantially lower maximum concentration, reflecting the cumulative influence of diffusion and reaction.

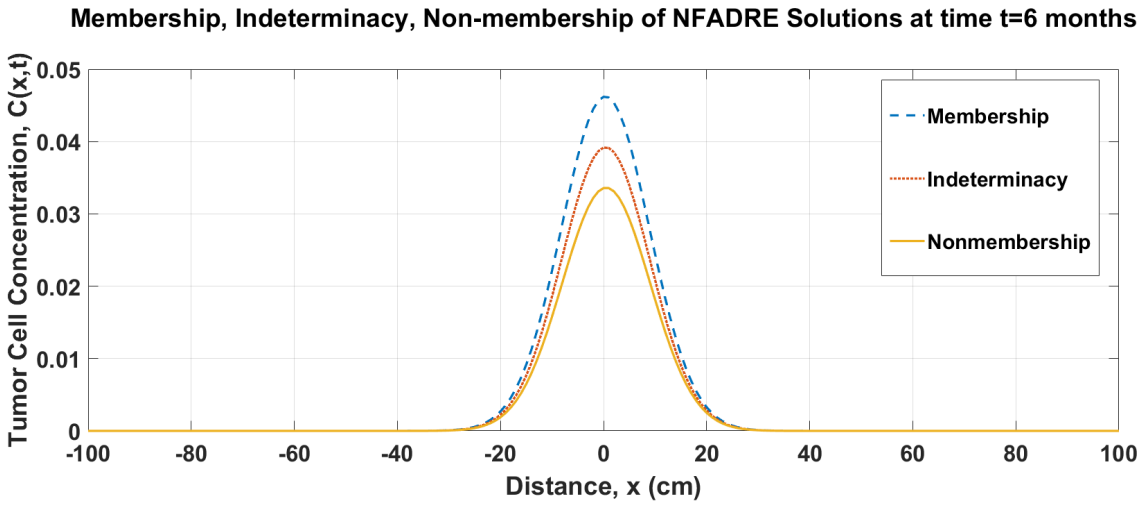

Figure 6: Cell Concentration using NFADRE at t=6 months for $\alpha = 0.6, \beta = 0.6, \gamma = 0.6$

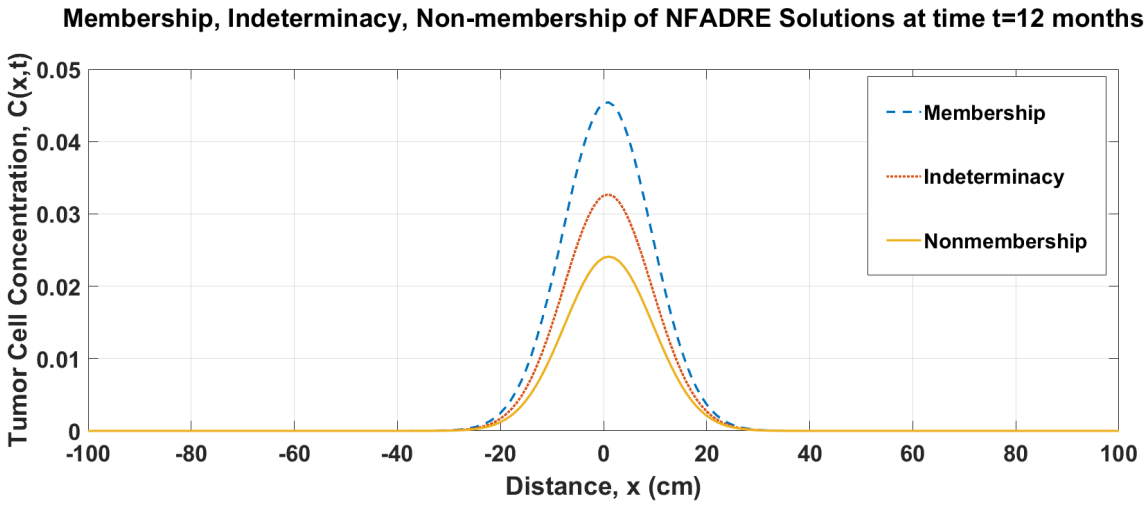

Figure 7: Cell Concentration using NFADRE at t=12 months for $\alpha = 0.6, \beta = 0.6, \gamma = 0.6$

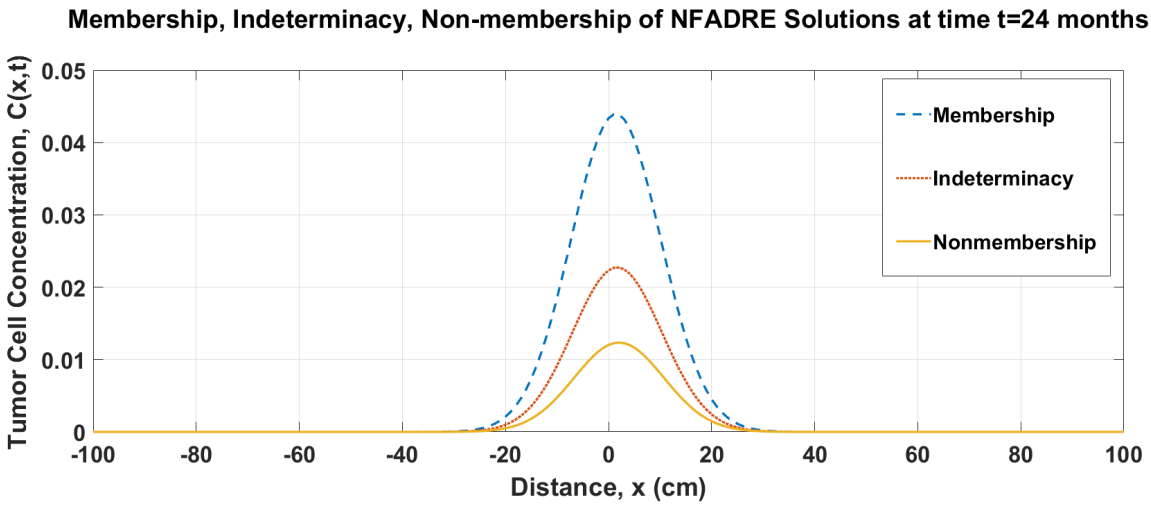

Figure 8: Cell Concentration using NFADRE at t=24 months for $\alpha = 0.6, \beta = 0.6, \gamma = 0.6$

The figures (6), (7) and (8) depict the spatial distributions of the membership, indeterminacy, and non-membership concentration profiles predicted by the proposed Neutrosophic Fuzzy Advection–Diffusion–Reaction Equation (NFADRE) for the (α, β, γ)-cut level (0.6,0.6,0.6) at t=6, 12, and 24 months, respectively. At t=6 months, the concentration profiles remain localized with relatively high amplitudes, indicating the early stage of tumor evolution. As time increases to t=12 months, the profiles undergo gradual spatial spreading accompanied by a reduction in peak concentration due to the combined effects of advection, diffusion, and reaction. By t=24 months, the concentration distributions become considerably broader with further attenuation of the peak values, reflecting the cumulative influence of diffusion-driven dispersion and reaction-induced decay. The membership function consistently exhibits the highest concentration, followed by the indeterminacy and non-membership functions, preserving the neutrosophic ordering throughout the simulation. Compared with the lower cut level (0.3,0.3,0.3), the (0.6,0.6,0.6)-cut yields a narrower uncertainty band, indicating reduced uncertainty and greater confidence in the predicted tumor concentration. The smooth and physically consistent evolution of all three neutrosophic components demonstrates the accuracy, stability, and robustness of the proposed numerical scheme for simulating tumor growth under uncertainty.

This demonstrates that the Neutrosophic Fuzzy model provides a more realistic representation by distinguishing clear, uncertain, and opposing states, whereas the conventional fuzzy model treats uncertainty implicitly through complementary membership and non-membership alone.

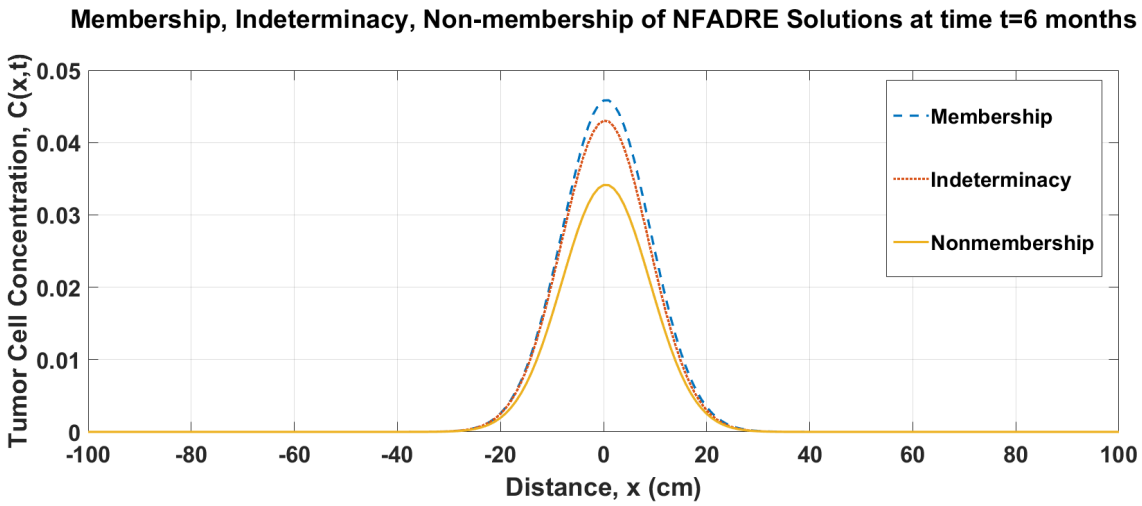

Figure 9: Cell Concentration using NFADRE at t=6 months for $\alpha = 0.9, \beta = 0.9, \gamma = 0.9$

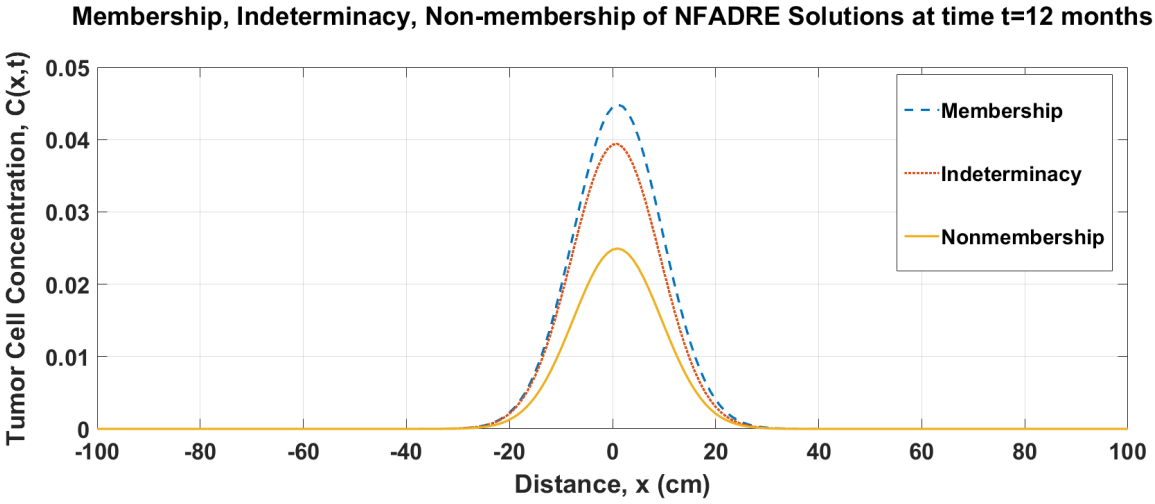

Figure 10: Cell Concentration using NFADRE at t=12 months for $\alpha = 0.9, \beta = 0.9, \gamma = 0.9$

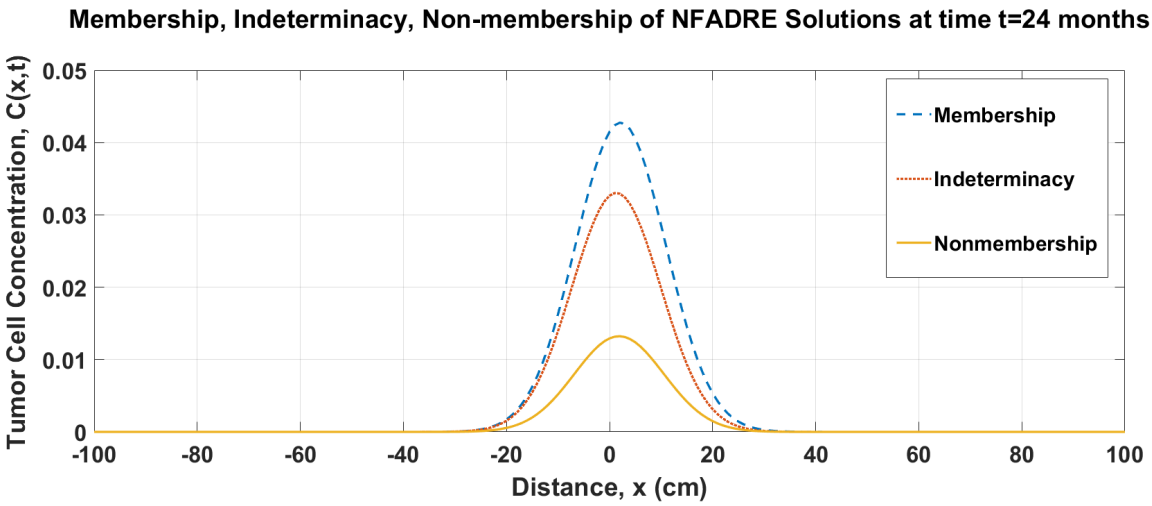

Figure 11: Cell Concentration using NFADRE at t=24 months for $\alpha = 0.9, \beta = 0.9, \gamma = 0.9$

Figures (9), (10) and (11) show the numerical results for the highest cut level, $(\alpha, \beta, \gamma) = (0.9, 0.9, 0.9)$. As expected, the transport mechanisms continue to govern the evolution of the tumor concentration in the same physical manner. The concentration profile shifts gradually in the direction of advection, spreads due to diffusion, and decreases continuously under the influence of the reaction process. Nevertheless, the membership, indeterminacy, and non-membership concentration profiles become much closer to one another, producing the narrowest uncertainty region among all simulated cases. This behavior indicates that increasing the (α, β, γ)-cut level reduces the interval width associated with the neutrosophic parameters and consequently yields more precise concentration predictions. The preservation of smooth concentration profiles and the absence of numerical instabilities further demonstrate the robustness of the proposed numerical algorithm.

A comparison of all three (α, β, γ)-cut levels reveals that the underlying physical behavior of the tumor remains unchanged regardless of the degree of uncertainty. In every case, advection transports the concentration profile in the prescribed flow direction, diffusion gradually broadens the spatial distribution, and the reaction term continuously decreases the overall concentration. The principal effect of varying the (α, β, γ)-cut level is therefore not to alter the physical dynamics but to modify the extent of uncertainty associated with the solution. Lower cut levels produce wider neutrosophic intervals because a larger range of admissible parameter values is considered, whereas higher cut levels generate narrower intervals corresponding to increased certainty in the model parameters. This progressive reduction of uncertainty demonstrates the consistency of the proposed neutrosophic formulation and highlights its capability to represent different confidence levels within a unified mathematical framework.

Overall, the numerical results verify that the proposed NFADRE successfully integrates advection, diffusion, reaction, and neutrosophic uncertainty into a single computational

model. The explicit finite difference scheme accurately captures the evolution of tumor concentration while preserving numerical stability, consistency, and convergence. Furthermore, the neutrosophic representation provides additional information beyond deterministic and classical fuzzy models by simultaneously quantifying membership, indeterminacy, and non-membership, thereby offering a more realistic and flexible framework for uncertainty-aware tumor growth prediction.

5. UNCERTAINTY ANALYSIS

To assess the influence of parameter uncertainty on the proposed model, an uncertainty analysis is performed for the neutrosophic transport and reaction coefficients. The uncertainty associated with the advection velocity, diffusion coefficient, and reaction coefficient is quantified by determining their interval bounds at the different membership, indeterminacy and non-membership levels. The resulting uncertainty bands provide a quantitative measure of the variability associated with the model parameters and illustrate the capability of the proposed NFADRE to produce reliable predictions under different levels of uncertainty.

Let $\tilde{P}$ denote an uncertain model parameter, where $\tilde{P} \in \{\tilde{u}, \tilde{D}, \tilde{\lambda}\}$, and let $P \in \{u, D, \lambda\}$ denote its corresponding deterministic value respectively. In the proposed framework, each uncertain parameter is represented by a triangular neutrosophic fuzzy number to account for the inherent uncertainty. Suppose that the relative uncertainty associated with a parameter $\tilde{P}$ is $\mu \times 100\%$, where $\mu \in (0, 1)$. Then the corresponding uncertainty interval is defined as $P \in [P - \mu P, P + \mu P]$ or equivalently, $P \in [(1 - \mu)P, (1 + \mu)P]$, where P denotes the deterministic value of the parameter and μ represents its relative uncertainty.

Table 1: Bounds for Flow velocity($\tilde{u}$), diffusion coefficient ($\tilde{D}$) and reaction coefficient ($\tilde{\lambda}$) in the error defined membership fuction.

Degree of membership	Bounds of $\tilde{u}$	Bounds of $\tilde{D}$	Bounds of $\tilde{\lambda}$
0.3	[0.3u, 2u-0.3u]	[0.75D+0.075D, 1.25D-0.075D]	[0.015λ, 0.1λ-0.015λ]
0.6	[0.6u, 2u-0.6u]	[0.75D+0.15D, 1.25D-0.15D]	[0.03λ, 0.1λ-0.03λ]
0.9	[0.9u, 2u-0.9u]	[0.75D+0.225D, 1.25D-0.225D]	[0.045λ, 0.1λ-0.045λ]

In an intuitionistic fuzzy set A, which is defined on a universe X, characterized by a membership function $(\mu_A(x))$ and a non-membership function $(\nu_A(x))$ satisfying $(0 \leq \mu_A(x) + \nu_A(x) \leq 1)$ for all $x \in X$. The associated hesitancy degree, representing the inherent uncertainty in the information, is given by $\pi_A(x) = 1 - \mu_A(x) - \nu_A(x)$. To regulate this uncertainty, restrictions are imposed on the membership and non-membership functions through parameters $(\alpha, \beta \in [0, 1])$. This leads to the

Table 2: Bounds for Flow velocity($\tilde{u}$), diffusion coefficient ($\tilde{D}$) and reaction coefficient ($\tilde{\lambda}$) in the error defined non-membership fuction.

Degree of non-membership	Bounds of $\tilde{u}$	Bounds of $\tilde{D}$	Bounds of $\tilde{\lambda}$
0.3	[u-0.15u, u+0.15u]	[D-0.225D, D+0.225D]	[λ-0.255λ, λ+0.255λ]
0.6	[u-0.3u, u+0.3u]	[D-0.45D, D-0.45D]	[λ-0.51λ, λ-0.51λ]
0.9	[u-0.45u, u+0.45u]	[D-0.675D, D+0.675D]	[λ-0.765λ, λ+0.765λ]

(α, β)-cut of an intuitionistic fuzzy set as $(A_{\alpha,\beta} = x \in X \mid \mu_A(x) \geq \alpha, \nu_A(x) \leq \beta)$. The (α, β)-cut therefore represents the subset of elements satisfying the prescribed bounds on membership and non-membership degrees, effectively controlling the uncertainty since $(\pi_A(x) \leq 1 - \alpha - \beta)$. For the hesitancy degree to remain non-negative, the condition $(\alpha + \beta \leq 1)$ must be satisfied; otherwise, if $(\alpha + \beta > 1)$, the resulting negative hesitancy contradicts the fundamental definition of uncertainty in intuitionistic fuzzy theory. Therefore, when the hesitancy function is defined based on error, it is not possible to assign meaningful bounds to parameters such as the flow velocity $(\tilde{u})$ and diffusion coefficient $(\tilde{D})$, because the resulting uncertainty representation becomes mathematically inconsistent and invalid.

In the above graphical representation of the problem, we have considered three cases for the degrees of membership and non-membership, which are $(0.3, 0.3), (0.6, 0.6)$ and $(0.9, 0.9)$. Therefore, the degree of hesitancy is 0.4 for the 1st case and undefined in the other two cases for Intuitionistic fuzzy model.

Table 3: Bounds for Flow velocity($\tilde{u}$), diffusion coefficient ($\tilde{D}$) and reaction coefficient ($\tilde{\lambda}$) in the error defined hesitancy fuction of intuitionistic fuzzy model.

Degree of hesitancy	Bounds of $\tilde{u}$	Bounds of $\tilde{D}$	Bounds of $\tilde{\lambda}$
0.4	[u-0.1u, u+0.1u]	[D-0.2D, D+0.2D]	[λ-0.06λ, λ+0.06λ]

Finally, we get an uncertainty left bound and right bound of 10% for flow velocity, 20% for diffusion coefficient and 6% for reaction coefficient, as shown in the table (3) using the fuzzy mathematics uncertainty quantification method[29] by extending it for intuitionistic fuzzy model. This shows that the intuitionistic fuzzy model restrict the representation of uncertainty in complex real world systems.
Unlike intuitionistic fuzzy sets, the degrees of membership, indeterminacy and

non-membership components of neutrosophic fuzzy model are not constrained by the condition $(\alpha + \beta + \gamma) = 1$. Instead they can vary independently within a broader range $0 \leq (\alpha + \beta + \gamma) \leq 3$. This flexibility allows neutrosophic fuzzy models to handel incomplete, inconsistent, and indeterminate information more effectively. For neutrosophic fuzzy model we have considered the degree of indeterminacy $0.3, 0.6$ and 0.9 to represent low, moderate and high uncertain scenarios.

Table 4: Bounds for Flow velocity($\tilde{u}$), diffusion coefficient ($\tilde{D}$) and reaction coefficient ($\tilde{\lambda}$) in the error defined indeterminacy fuction of neutrosophic fuzzy model.

Degree of indeterminacy	Bounds of $\tilde{u}$	Bounds of $\tilde{D}$	Bounds of $\tilde{\lambda}$
0.3	[u-0.075u, u+0.075u]	[D-0.15D, D+0.15D]	[λ-0.045λ, λ+0.045λ]
0.6	[u-0.15u, u+0.15u]	[D-0.3D, D+0.3D]	[λ-0.09λ, λ+0.09λ]
0.9	[u-0.225u, u+0.225u]	[D-0.45D, D+0.45D]	[λ-0.135λ, λ+0.135λ]

For neutrosophic fuzzy model, we get an uncertainty left bound and right bound of 7.5% for flow velocity, 15% for diffusion coefficient and 4.5% for reaction coefficient when the degree of indeterminacy is 0.3, as shown in the table (4) using the uncertainty quantification method, used in[29] by applying it for neutrosophic fuzzy model. Similarly, for the other two cases, we get an uncertainty left bound and right bound of 15% for flow velocity, 30% for diffusion coefficient and 9% for reaction coefficient when the degree of indeterminacy is 0.6 and uncertainty left bound and right bound of 22.5% for flow velocity, 45% for diffusion coefficient and 13.5% for reaction when the degree of indeterminacy is 0.9, as shown in the table (4). As in neutrosophic fuzzy model, the degree of indeterminacy can independently vary within the range of [0,1], therefore the value of uncertainty for flow velocity, diffusion coefficient and reaction coefficient would lie within the range of $[0, 25]\%$, $[0, 50]\%$ and [0,15%] for the considered example.

The uncertainty analysis demonstrates that the proposed neutrosophic framework effectively quantifies the variability associated with the governing model parameters. The quantified interval bounds provide a realistic range of admissible parameter values, enabling a systematic assessment of their influence on the predicted tumor concentration. These results confirm that the proposed formulation offers a reliable and flexible approach for incorporating uncertainty into the advection–diffusion–reaction model while preserving numerical consistency.

6. CONCLUSIONS AND FUTURE WORK

This study presented a novel neutrosophic advection–diffusion–reaction (ADR) model for tumor growth in which the diffusion coefficient and reaction parameter were represented by triangular neutrosophic numbers to explicitly account for uncertainty and indeterminacy in biological systems. Unlike conventional deterministic, fuzzy, and intuitionistic fuzzy formulations, the proposed model independently incorporates truth-membership, indeterminacy-membership, and falsity-membership, thereby providing a more comprehensive mathematical representation of the uncertainty associated with tumor progression. The neutrosophic ADR model was transformed into an equivalent parametric form using the (α, β, γ)-cut representations and solved numerically using an efficient finite difference upwind scheme. Furthermore, the numerical experiments illustrated the influence of neutrosophic uncertainty on tumor evolution and showed that independent modeling of indeterminacy yields additional insight into tumor dynamics that cannot be captured by classical, fuzzy, or intuitionistic fuzzy models. Consequently, the proposed framework provides a more realistic and flexible mathematical tool for investigating tumor growth under uncertain biological conditions and contributes to the growing field of uncertainty-aware mathematical oncology.

Although the proposed model represents a significant step toward incorporating neutrosophic uncertainty into tumor-growth modeling, several research directions remain open. Future studies may extend the present formulation to multidimensional and patient-specific tumor-growth models involving heterogeneous tissue properties, and complex tumor microenvironments. The incorporation of nonlinear reaction kinetics, angiogenesis, immune-cell interactions, drug transport, chemotherapy, radiotherapy, and immunotherapy would further enhance the biological realism of the model.In addition, advanced numerical techniques such as adaptive finite difference methods, finite element methods, finite volume methods, spectral methods, and mesh-free approaches may be investigated to improve computational efficiency and accuracy for large-scale simulations. Parameter estimation and model calibration using experimental or clinical imaging data could facilitate patient-specific predictions and support personalized treatment planning. Furthermore, integrating neutrosophic mathematical models with machine learning and artificial intelligence may provide robust predictive frameworks for uncertainty quantification, treatment optimization, and clinical decision support. These extensions have the potential to establish neutrosophic mathematical modeling as a powerful framework for addressing uncertainty in complex biomedical systems and advancing the application of computational mathematics in cancer research.

REFERENCES

[1] ALABDRABALNABI, A. S., AND ALI, I. Stability analysis and simulations of tumor growth model based on system of reaction–diffusion equation in two-dimensions. *AIMS Math 9*, 5 (2024), 11560–11579.

[2] ALLAHVIRANLOO, T. Difference methods for fuzzy partial differential equations. *Computational Methods in Applied Mathematics 2*, 3 (2002), 233–242.

[3] ATANASSOV, K. T. Intuitionistic fuzzy sets. *Fuzzy Sets and Systems 20*, 1 (1986), 87–96.

[4] BUCKLEY, J. J., AND FEURING, T. Introduction to fuzzy partial differential equations. *Fuzzy sets and systems 105*, 2 (1999), 241–248.

[5] BYRNE, H. M. Dissecting cancer through mathematics: from the cell to the animal model. *Nature Reviews Cancer 10*, 3 (2010), 221–230.

[6] CHAKRABORTY, A., MONDAL, S. P., AHMADIAN, A., SENU, N., ALAM, S., AND SALAHSHOUR, S. Different forms of triangular neutrosophic numbers, de-neutrosophication techniques, and their applications. *Symmetry 10*, 8 (2018), 327.

[7] CHEN-CHARPENTIER, B. M., AND KOJOUHAROV, H. V. An unconditionally positivity preserving scheme for advection–diffusion reaction equations. *Mathematical and computer modelling 57*, 9-10 (2013), 2177–2185.

[8] CRUYWAGEN, G. C., WOODWARD, D. E., TRACQUI, P., BARTOO, G. T., MURRAY, J., AND ALVORD, E. C. The modelling of diffusive tumours. *Journal of Biological Systems 3*, 04 (1995), 937–945.

[9] FISHER, R. A. The wave of advance of advantageous genes. *Annals of eugenics 7*, 4 (1937), 355–369.

[10] GAZI, K. H., BISWAS, A., SINGH, P., RAHAMAN, M., MAITY, S., MAHATA, A., AND MONDAL, S. P. A comprehensive literature review of fuzzy differential equations with applications. *Journal of fuzzy extension and applications 6*, 1 (2025), 134–161.

[11] GEORGIEVA, A., CHOLAKOV, S. I., AND SPASOVA, M. A new double fuzzy integral transform for solving an advection–diffusion equation. *Axioms 14*, 4 (2025), 240.

[12] HARPOLD, H. L., ALVORD JR, E. C., AND SWANSON, K. R. The evolution of mathematical modeling of glioma proliferation and invasion. *Journal of Neuropathology & Experimental Neurology 66*, 1 (2007), 1–9.

[13] KAMAL, B., KHALID, H. E., SALAMA, A., AND EL-BAGHDADY, G. I. Finite difference method for neutrosophic fuzzy second order differential equation under generalized hukuhara differentiability. *Neutrosophic Sets and Systems 58*, 1 (2023), 19.

[14] KERMANI, M. A., AND SABURI, F. Numerical method for fuzzy partial differential equations. *Applied Mathematical Sciences 1*, 27 (2007), 1299–1309.

[15] KHALIQ, R., IQBAL, P., BHAT, S. A., AND SHEERGOJRI, A. R. A fuzzy mathematical model for tumor growth pattern using generalized hukuhara derivative and its numerical analysis. *Applied Soft Computing 118* (2022), 108467.

[16] KHALIQ, R., IQBAL, P., BHAT, S. A., SINGH, R., JAIN, S., AND AGARWAL, P. Generalized hukuhara derivative approach for gompertz tumor growth with allee effect under fuzzy environment. *Journal of fuzzy extension and applications 4*, 4 (2023), 246–256.

[17] MAN, S., SAW, B., AND HAZRA, S. An explicit method for solving intuitionistic fuzzy heat equation. *Adv. Fuzzy Math.(AFM) 16* (2021), 27–39.

[18] QAYYUM, M., NAYAB, S., KHAN, O., HASSANI, M. K., AND AKGÜL, A. A hybrid computational framework for fractional cancer diffusion models in uncertain settings. *Scientific Reports 15*, 1 (2025), 33858.

[19] RIVAZ, A., AZIZIAN, M., KAMYAD, A. V., AND ZADEH, S. Z. A full fuzzy generalized mathematical model of tumor growth and its analysis. *Journal of intelligent & fuzzy systems 35*, 6 (2018), 6453–6460.

[20] SEIKKALA, S. On the fuzzy initial value problem. *Fuzzy sets and systems 24*, 3 (1987), 319–330.

[21] SMARANDACHE, F. Neutrosophy: neutrosophic probability, set, and logic: analytic synthesis & synthetic analysis.

[22] SMARANDACHE, F. Neutrosophic set is a generalization of intuitionistic fuzzy set, inconsistent intuitionistic fuzzy set (picture fuzzy set, ternary fuzzy set), pythagorean fuzzy set, spherical fuzzy set, and q-rung orthopair fuzzy set, while neutrosophication is a generalization of regret theory, grey system theory, and three-ways decision (revisited). *Journal of new theory*, 29 (2019), 1–31.

[23] SWANSON, K. R., ALVORD JR, E. C., AND MURRAY, J. D. A quantitative model for differential motility of gliomas in grey and white matter. *Cell proliferation 33*, 5 (2000), 317–329.

[24] SWANSON, K. R., BRIDGE, C., MURRAY, J., AND ALVORD JR, E. C. Virtual and real brain tumors: using mathematical modeling to quantify glioma growth and invasion. *Journal of the neurological sciences 216*, 1 (2003), 1–10.

[25] TRACQUI, P. From passive diffusion to active cellular migration in mathematical models of tumour invasion. *Acta biotheoretica 43*, 4 (1995), 443–464.

[26] TSEGA, E. G. Numerical solution of two-dimensional nonlinear unsteady advection-diffusion-reaction equations with variable coefficients. *International Journal of Mathematics and Mathematical Sciences 2024*, 1 (2024), 5541066.

[27] WANG, H., SMARANDACHE, F., ZHANG, Y., AND SUNDERRAMAN, R. *Single valued neutrosophic sets*. Infinite study, 2010.

[28] ZADEH, L. A. Fuzzy sets. *Information and control 8*, 3 (1965), 338–353.

[29] ZHANG, Z., AND VALEO, C. Fuzzy-based input method for uncertainty quantification in a deterministic model comparison with chatgpt for peak flow prediction. *Journal of Hydrology X* (2025), 100208.

[30] ZUREIGAT, H., ALSHAMMARI, S., ALSHAMMARI, M., AL-SMADI, M., AND AL-SAWALLAH, M. M. An in-depth examination of the fuzzy fractional cancer tumor model and its numerical solution by implicit finite difference method. *Plos one 19*, 12 (2024), e0303891.

[31] ZUREIGAT, H., BAWANEH, S., AL-KHATEEB, A., AND NUSAIRAT, N. A comprehensive study on exact and numerical methods for solving the neutrosophic fuzzy advection–diffusion equation. *Journal of Mathematics 2026*, 1 (2026), 6881602.